Articles

Stopped-Flow Analyses on the Reaction of Ascorbate with Cytochrome b_{561} Purified from Bovine Chromaffin Vesicle Membranes†

Tadakazu Takigami,‡ Fusako Takeuchi,‡ Masashi Nakagawa,‡ Toshiharu Hase,§ and Motonari Tsubaki*,‡,§,||

Department of Life Science, Graduate School and Faculty of Science, Himeji Institute of Technology, Kamigoori-cho, Akou-gun, Hyogo 678-1297, Japan, Institute for Protein Research, Osaka University, Suita, Osaka 565-0871, Japan, and Department of Molecular Science, Graduate School of Science and Technology, Kobe University, Nada-ku, Kobe, Hyogo 657-8501, Japan

Received August 29, 2002; Revised Manuscript Received May 16, 2003

ABSTRACT: Cytochrome b_{561} in adrenal chromaffin vesicle membranes conveys electron equivalents from extravesicular ascorbate to the intravesicular monodehydroascorbate radical. We conducted a stopped-flow study on the reaction of ascorbate with purified cytochrome b_{561} in the detergent-solubilized state for the first time. The time course of the reduction of oxidized cytochrome b_{561} with ascorbate could not be fitted with a single exponential but with a linear combination of at least four exponential functions. This result is consistent with the notion that cytochrome b_{561} contains two hemes *b*, each having a distinct redox potential and a function upon reactions with ascorbate and monodehydroascorbate radical. The fastest phase, which was assigned to the first one-electron donation from ascorbate to heme *b* on the extravesicular side, was further analyzed by transient phase kinetics employing a two-step bi−uni sequential ordered mechanism. The result showed $K_s = 2.2$ mM for ascorbate at pH6.0. At a region below pH5.5, there was a significant lag before the reduction of hemes *b* occurred. This time lag was interpreted as due to a pH-dependent transient state before the first electron transfer to take place. The fastest phase was completely lost by *N*-carbethoxylation of heme-coordinating histidyl residues (His88 and His161) and Lys85 upon treatment with diethylpyrocarbonate. The presence of ascorbate during the treatment inhibited the *N*-carbethoxylation of the histidyl residues and, thereby, restored the final reduction level of hemes *b*. But the reduction rate was still only one-twentieth of the native form. This result suggested an important role of the conserved Lys85 for the interaction with ascorbate.

Vitamin C (L-ascorbic acid; AsA[1]) is essential for many enzymatic reactions, in which it serves to maintain prosthetic metal ions in their reduced forms. The brain and neuroendocrine tissues have the highest AsA levels of any organ system (*1*) because of the presence of a specific AsA transporter system in neurons or neuroendocrine cells (*2*) that maintain the steep intra/extracellular concentration gradient. In neurosecretory vesicles, such as adrenomedullary chromaffin vesicles and pituitary neuropeptide secretory vesicles, intravesicular AsA is believed to function as the electron donor for copper-containing monooxygenases, such as dopamine β-hydroxylase and peptidylglycine α-amidating monooxygenase (*3*, *4*). Upon these monooxygenase reactions, the monodehydroascorbate (MDA) radical is produced within the vesicles by univalent oxidation of AsA (*5*). Since neither AsA nor the MDA radical can pass through the vesicle membranes (*6*−*8*), it is believed that the intravesicular MDA radical is reduced back to AsA by membrane-spanning cytochrome b_{561} and subsequently the oxidized cytochrome b_{561} is reduced by AsA on the extravesicular side (i.e., the cytosolic side). Thus, cytochrome b_{561} acts as a neuroendocrine-specific transmembrane electron carrier from very primitive animal Plathelminthes (*9*) to higher vertebrates including humans (*10*).

Cytochrome b_{561} is a highly hydrophobic hemoprotein (*11*, *12*) with a molecular mass of 29 kDa (*12*) containing two distinct heme *b* centers (*13*). In the oxidized state, one heme *b* showed a usual low-spin EPR signal ($g_z = 3.14$), and the other gave a highly anisotropic low-spin EPR signal ($g_z = 3.70$) (*13*−*15*). On the basis of comparison of the deduced amino acid sequences, we have proposed a plausible structural model of cytochrome b_{561} (*16*), by extending the model of Degli Esposti et al. (*17*). Although Srivastava et al. proposed previously a five-transmembrane segment model

† This work was supported by Grants-in-Aid for Scientific Research on Priority Areas (Comprehensive Promotion Study of Brain; 12050236 to M.T.) and (C) (12680659 and 14580676 to M. T.) from the Japanese Ministry of Education, Science, Sports and Culture and was supported partly by CREST, JST.

* Corresponding author. Address: Department of Molecular Science, Graduate School of Science and Technology, Kobe University, 1-1 Rokkodai-cho, Nada-ku, Kobe, Hyogo 657-8501, Japan. Fax: +81-78-803-6582. Tel: +81-78-803-6582. E-mail: mtsubaki@kobe-u.ac.jp.

‡ Himeji Institute of Technology.

§ Osaka University.

|| Kobe University.

[1] Abbreviations: AsA, ascorbate; MDA, monodehydroascorbate; DEPC, diethyl pyrocarbonate, MALDI-TOF, matrix-assisted laser desorption/ionization-time-of-flight.

10.1021/bi0267588 CCC: $25.00
Published on Web 06/20/2003

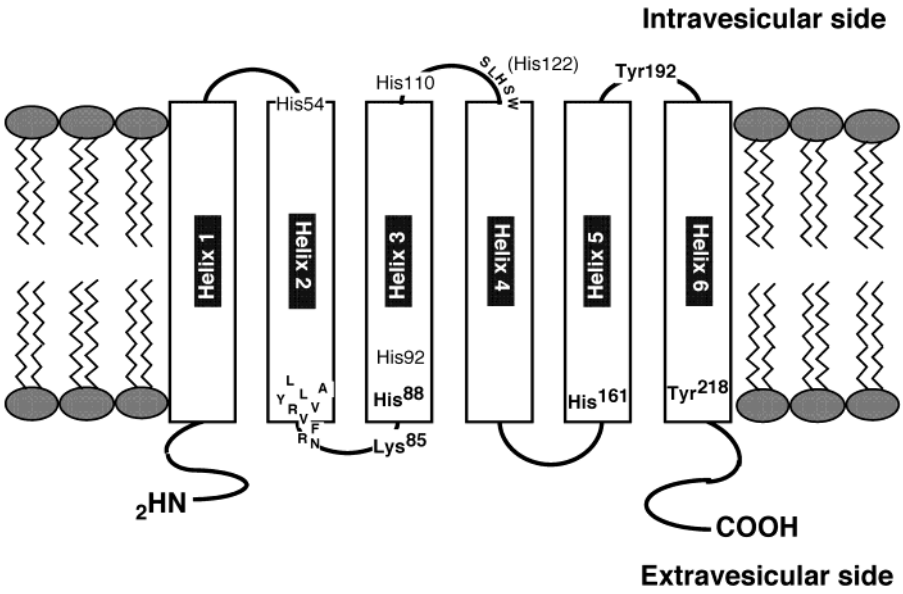

FIGURE 1: Transmembrane structural model of bovine cytochrome b_{561}. Two fully conserved sequences (^{69}ALLVYRVFR^{77} and ^{120}SLHSW^{124}) and six conserved histidyl residues (His54, His88, His92, His110, His122, and His161) are indicated. His54 and His122 are likely the heme axial ligands on the intravesicular side, whereas His161 and His88 are considered as the heme axial ligands on the extravesicular side. Three major (Lys85, His88, and Hi161) and two minor (Tyr192 and Tyr218) modification sites with DEPC are indicated in bold face.

(*18*, *19*) based on the heme content analysis (1 heme *b*/monomer) (*20*) and the topological accessibility of antibodies and Pronase (*21*), the model had a difficulty to accommodate two heme prosthetic groups. On the other hand, Kamensky et al. proposed that cytochrome b_{561} in chromaffin vesicles forms a dimer, with one heme *b* per monomer and one heme *b* residing between the interfaces of two monomers (*22*). However, there is no experimental evidence to suggest the dimer fomation in the vesicle membranes.

In our model (Figure 1), there are two fully conserved regions in the sequences; the first one (^{69}ALLVYRVFR^{77}) is located on the extravesicular side of α-helical segment, and the second one (^{120}SLHSW^{124}) is located in an intravesicular loop connecting two α-helical segments (*16*). These conserved sequences may form a part of the binding sites for extravesicular AsA and the intravesicular MDA radical, respectively (*16*). Therefore, the two hemes *b* might be located on each side of the vesicular membranes in close contact with these binding sites, respectively (*16*). Indeed our pulse radiolysis analysis showed that the two heme *b* centers have distinct roles for the electron donation to the MDA radical and the electron acceptance from AsA, respectively (*23*). We found further that the electron accepting ability from AsA was selectively destroyed by the treatment of oxidized cytochrome b_{561} with diethylpyrocarbonate (DEPC). However, the electron donating activity from the reduced heme *b* center to the MDA radical was retained (*24*). Matrix-assisted laser desorption/ionization-time-of-flight (MALDI-TOF) mass spectrometric analyses revealed that two fully conserved histidyl residues (His88 and His161), possible heme ligands on the extravesicular side, and Lys85 were the modification sites with DEPC (*24*). Further, the electron accepting ability from AsA could be protected by the presence of AsA during the DEPC treatment, suggesting the AsA-binding site on the extravesicular side (*25*).

The kinetics of the reactions between cytochrome b_{561} and AsA or MDA radical has been studied in some detail for chromaffin vesicles (*5*, *26*) and for their ghosts (*27*−*32*). It was reported that reduction of cytochrome b_{561} in chromaffin vesicles by external AsA exhibited Michaelis−Menten kinetics with the apparent K_m of around 300 μM (*26*, *27*) or 4 mM (*32*). However, no detailed study has been reported for the reaction of AsA with purified cytochrome b_{561}, except for our pulse radiolysis studies (*23*, *24*).

In the present study, we conducted a stopped-flow study on the reaction of AsA with purified cytochrome b_{561} in the detergent-solubilized state for the first time. We have succeeded to analyze kinetics of the multiphase electron-transfer reaction. Further, effect of the treatment of cytochrome b_{561} with DEPC on the electron-transfer reaction was examined.

MATERIALS AND METHODS

Purification of Cytochrome b_{561}. Cytochrome b_{561} was purified from bovine adrenal medulla to a homogeneous state, as described previously (*13*). The purity of cytochrome b_{561} was analyzed with visible absorption spectra, heme content analysis, and SDS−polyacrylamide gel electrophoresis (*13*). All other reagents were commercially obtained as the analytical grade. The concentration of cytochrome b_{561} was determined using a millimolar extinction coefficient of 267.9 mM^{-1} cm^{-1} at 427 nm in the reduced state (*13*).

Modification of Cytochrome b_{561} with DEPC. Concentrated cytochrome b_{561} solution was acidified to pH 6.5 by adding 0.5 M potassium phosphate buffer (pH 6.0) and was oxidized by stepwise additions of potassium ferricyanide solution (100 mM). Complete oxidation was checked with visible absorption spectroscopy. The oxidized cytochrome b_{561} was gel-filtered through a PD-10 column (Amersham Pharmacia Biotech) equilibrated with 50 mM potassium phosphate buffer (pH 6.0) containing 1.0% (w/v) octyl β-glucoside and was then diluted with the same buffer to an appropriate concentration. The diluted sample was treated with DEPC

for 30 min, as previously described (*24*). The DEPC treatment of cytochrome b_{561} in the presence of 20 mM AsA was done similarly. The DEPC-treated samples were gel-filtered through a PD-10 column equilibrated with 50 mM potassium phosphate buffer (pH 6.0) containing 1.0% (w/v) octyl β-glucoside to remove unreacted DEPC. The DEPC-treated cytochrome b_{561} sample was then analyzed for the reactivity with AsA with a Shimadzu UV-2400PC spectrophotometer (Kyoto, Japan). Finally, the sample was fully reduced with sodium dithionite, and its absorption spectrum was recorded to check the integrity of the heme moiety.

Stopped-Flow Measurements. Rapid kinetic measurements were carried out using an SX.18MV stopped-flow spectrometer (Applied Photophysics, Leatherhead, U.K.). One chamber of the apparatus contained oxidized cytochrome b_{561} (2.0 μM) in 50 mM sodium acetate (pH 5.0 and 5.5) or 50 mM potassium phosphate buffer (pH 6.0, 6.5, 7.0, or 7.5) containing 1.0% octyl β-glucoside. The other chamber contained a test concentration of sodium ascorbate (AsA) in the same buffer. The temperature of both chambers and the sample holder was maintained at 20 °C with a connection to a thermobath. The mixing was carried out with 1:1 ratio, and cytochrome b_{561} reduction was followed spectrophotometrically at 427 nm. Data points were collected in every 5 ms from 0 to 1 s and in every 0.25 s from 1 to 50 s. The data obtained were analyzed with following procedures.

Analysis of the Stopped-Flow Data.The time courses of the absorbance change were fitted by use of a nonlinear least-squares method of Igor Pro (v.3.1) with a single (or a linear combination of) exponential equation

$$A = A_0 + (A_1 - A_0)\{1 - \exp(-k_{app}t)\} \quad (1)$$

$$A = A_0 + (A_1 - A_0)\{1 - \exp(-k_{app1}t)\} + \cdots + (A_n - A_{n-1})\{1 - \exp(-k_{appn}t)\} \quad (2)$$

For the analyses based on eq 2, we used a macro program for Igor Pro to obtain a first rough estimation for the values, A_0, $A_1 - A_0$, ... $A_n - A_{n-1}$, $k_{app1} > k_{app2} > \ldots > k_{appn}$, according to the following protocol. We assumed that, in the slower time domain where the faster processes already completed, only the slowest process was dominant. Therefore, this process could be fitted with a single-exponential equation, like eq 1. This led a rough estimation of $A_n - A_{n-1}$ and k_{appn}. Subtraction of the nth exponential function from the original data allowed the estimation of the $(n-1)$th term, the second slowest process, in a similar manner. After repeating similar procedures, we could complete the rough estimation for A_0, $A_1 - A_0$, ... $A_n - A_{n-1}$, k_{app1}, k_{app2}, ... k_{appn}. These roughly estimated values were then used as the starting values to fit the data based on the eq 2. The entire procedure gave a satisfactory fit to the original data.

The fastest phase, which was considered as the first one-electron donation reaction from AsA to the heme *b* center at the extravesicular side, was analyzed further according to a transient kinetic method based on a two-step bi−uni sequential ordered mechanism, as shown in eq 3:

$$E + S \underset{k_{-1}}{\overset{k_1}{\rightleftharpoons}} ES \underset{k_{-2}}{\overset{k_2}{\rightleftharpoons}} E^*(+P) \quad (3)$$

The apparent rate constants of the fastest phase (k_{app1}), expressed as units of inverse seconds (s^{-1}), were plotted against the AsA concentrations. The plots showed a saturation behavior at higher AsA concentrations and indicated that ES ↔ E*(+P) was much slower than E + S ↔ ES. In this case, k_{app1} could be expressed as the following expression:

$$k_{app1} = \frac{k_2([E] + [S])}{K_s + ([E] + [S])} + k_{-2} \quad (4)$$

where [E] and [S] denote the concentrations of E and S in equilibrium, respectively, and $K_s = k_{-1}/k_1$. In our present case, [E] could be neglected in comparison with [S], and further, [S] could be approximated to the initial concentrations of AsA. Closer examination of the plots showed that the k_{-2} could be neglected, and therefore, the Michaelis−Menten-type reaction (i.e., a rapid equilibrium between E + S ↔ ES) is operative. Finally, K_s and k_2 were determined using a least-squares method to fit the double reciprocal plots of the k_{app1} and the AsA concentrations.

At a lower pH region, we observed a significant time lag before the reduction of the heme *b* center occurred (see Results). This kind of unusual time courses could not be analyzed by the procedure described above. We, therefore, conducted a different approach by assuming the presence of an intermediate(s) before the ES complex formation. In actual analyses, we assumed following relaxation steps to describe the whole reduction process

$$AsA + b_{561} \rightleftarrows AsA\bullet b_{561} \rightleftarrows AsA\bullet b_{561}^* \rightleftarrows MDA\bullet b_{561}^{*-} \quad (5)$$

$$AsA + MDA\bullet b_{561}^{*-} \rightleftarrows AsA + b_{561}^{*-} \rightleftarrows AsA + MDA$$
$$AsA\bullet b_{561}^{*-} \rightleftarrows MDA\bullet b_{561}^{*2-} \quad (6)$$

where eq 5 denotes the first one-electron-transfer reaction and eq 6 indicates the second one-electron-transfer reaction. The asterisk indicates the activated form of cytochrome b_{561} after the binding of an AsA molecule to the AsA-binding site, and only within this form can the electron transfer from AsA to the heme *b* center at the extravesicular side take place. Under the assumption of this kind of multistep reversible reactions, the first one-electron-transfer reaction process (eq 5) could be treated with following three relaxations:

$$AsA + b_{561} \xrightarrow{k_3'} AsA\bullet b_{561} \xrightarrow{k_4'} AsA\bullet b_{561}^* \xrightarrow{k_5'} MDA\bullet b_{561}^{*-} \quad (7)$$

On the other hand, the relaxation process (eq 6) was further approximated to eq 6′ for the simplicity.

$$AsA + MDA\bullet b_{561}^{*-} \xrightarrow{k_6'} MDA + MDA\bullet b_{561}^{*2-} \quad (6')$$

In addition to these two major processes, there might be slow relaxation processes corresponding to a direct one-electron transfer from AsA to the heme *b* center on the intravesicular side and a reoxidation of the reduced heme *b* with MDA radical (see Discussion). We assumed that these slow processes corresponded to the slowest phase observed at pH 6.0 and 6.5, and therefore, these processes were treated as a

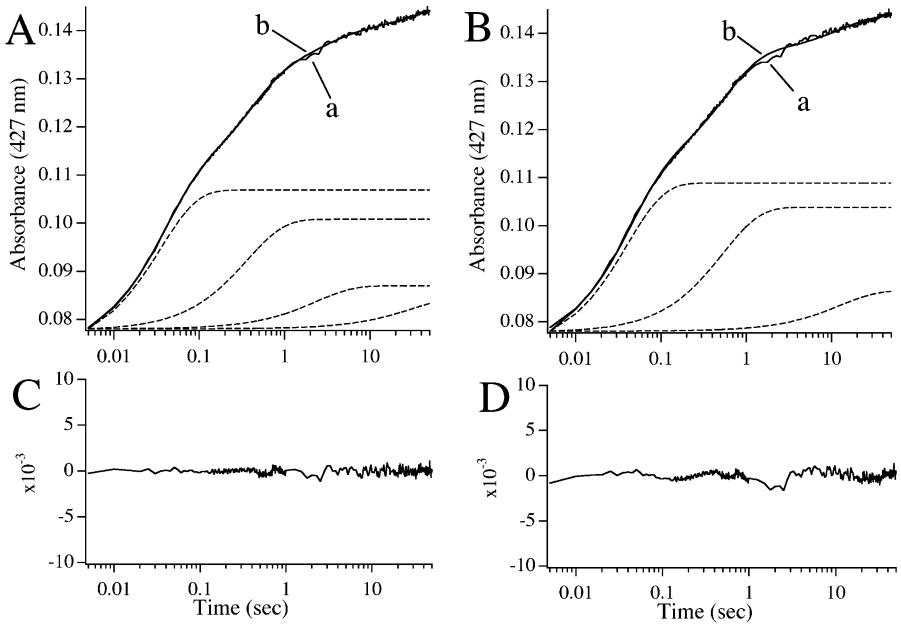

FIGURE 2: Time course of the reduction process of oxidized cytochrome b_{561} with AsA at pH 6.0 and its fitting analysis with exponential functions. Oxidized cytochrome b_{561} in 50 mM potassium phosphate (pH 6.0) buffer containing 1.0% octyl β-glucoside was mixed (1:1 in volume) with sodium AsA (16.0 mM) in the same buffer. Time course of the reduction was followed by absorbance change at 427 nm and is shown on a logarithmic time scale (traces a in panels A and B). The observed trace was fitted (traces b in panels A and B) either with four exponential functions (broken traces in panel A) or with three exponential functions (broken traces in panel B) using the procedure described in Materials and Methods. Parameters for the fitted four exponential functions (panel A) were as follows: $A_1 - A_0 = 46.3\%$ of total absorbance change, $k_{app1} = 28.6\ s^{-1}$; $A_2 - A_1 = 32.1\%$, $k_{app2} = 2.76\ s^{-1}$; $A_3 - A_2 = 12.5\%$, $k_{app3} = 0.429\ s^{-1}$; $A_4 - A_3 = 9.1\%$, $k_{app4} = 0.0321\ s^{-1}$. Parameters for the fitted three exponential functions (panel B) were as follows: $A_1 - A_0 = 50.3\%$, $k_{app1} = 24.89\ s^{-1}$; $A_2 - A_1 = 37.5\%$, $k_{app2} = 1.88\ s^{-1}$; $A_3 - A_2 = 12.2\%$, $k_{app3} = 0.0080\ s^{-1}$. Residuals (observed curve *minus* fitted curve) either with four (panel C) or three (panel D) exponential functions are also shown to clarify the validity of the fitting.

single relaxation process for the simplicity. The corrected trace, which was obtained by the subtraction of the slowest relaxation process from the original trace, was used for the next fitting procedure.

All three relaxation processes in eq 7 and one relaxation process in eq 6′ were treated as sequential first-order reactions, and the buildup of the MDA•b_{561}*$^{-}$ and MDA•b_{561}*$^{2-}$ species was fitted to the corrected trace assuming $k_3' > k_4' > k_5' \gg k_6'$. The estimated values were, then, used as the starting values for the final fitting to the observed trace, where eqs 6′ and 7 and the slowest single relaxation process were included. For the simplicity of the analyses, we further assumed that the final reduction level of the two heme centers were identical. The entire fitting approach was conducted for various AsA concentrations, and the results showed a satisfactory match (Figure 4A,B). A similar fitting approach was employed for the analyses of the data obtained at higher pH (i.e., pH 6.0 and 6.5). Then the apparent first-order rate constants (k_3', k_4', k_5', and k_6') were plotted against the AsA concentrations. Careful analyses of the plots showed that both k_4' and k_5' followed the hyperbolic nature against the AsA concentration (Figure 5). The curves were found to follow the multistep system (*33*) with a special case of $k_3, k_{-3} \gg k_4, k_{-4} \gg k_5, k_{-5}$, where we assumed a following eq 7′:

$$\text{AsA} + b_{561} \underset{k_{-3}}{\overset{k_3}{\rightleftharpoons}} \text{AsA}\bullet b_{561} \underset{k_{-4}}{\overset{k_4}{\rightleftharpoons}} \text{AsA}\bullet b_{561}{}^{*} \underset{k_{-5}}{\overset{k_5}{\rightleftharpoons}} \text{MDA}\bullet b_{561}{}^{*-} \quad (7)$$

Under this special case, k_5' could be expressed by the following eq 8:

$$k_5' = A + \frac{B[\text{AsA}]}{C + [\text{AsA}]} \quad (8)$$

In this equation, $A = k_{-5}$, $B = k_5K_4/(1 + K_4)$, and $C = 1/\{K_3(1 + K_4)\}$; where $K_3 = k_3/k_{-3}$, $K_4 = k_4/k_{-4}$, and [AsA] means the AsA concentration. In our experimental condition, k_{-5} and, therefore, the term A could be neglected. Least-squares fittings were conducted for the k_5' versus [AsA] plots for various pH.

RESULTS

Reduction of Cytochrome b_{561} with AsA at pH 6.0. Upon mixing of AsA (final 8.0 mM or 4.0 mM) with oxidized cytochrome b_{561} at pH 6.0, the absorbance at 427 nm (Soret band peak of the reduced form) showed a rapid increase, as shown in Figures 2 and 3. The time course, however, could not be fitted with a single-exponential function at all (Figure 2A). We found that a linear combination of at least four exponential functions was required to obtain a satisfactory fit (Figure 2A). In Figure 2B, a best fit using three exponential functions is also presented. Comparison of the residuals confirmed the requirement of four exponentials (Figure 2C,D). The result is consistent with our proposal that cytochrome b_{561} contains two hemes *b* centers, each having a distinct midpoint potential and a physiological role upon reactions with AsA and the MDA radical (*24*). Further, an internal electron transfer between the two heme *b* centers

Table 1: Statistics of the Fitted Parameters for the Reaction of Cytochrome b_{561} with Various Concentration of AsA at pH 6.0[a]

AsA (final)	first phase	second phase	third phase	fourth phase
8.0 mM				
k_{appn} (s^{-1})	32.02 ± 3.14	4.699 ± 1.916	0.7635 ± 0.3337	0.0507 ± 0.0137
$A_n - A_{n-1}$ (%)	42.51 ± 3.28	27.62 ± 4.95	20.26 ± 7.26	9.49 ± 0.75
4.0 mM				
k_{appn} (s^{-1})	22.56 ± 3.17	4.489 ± 2.572	0.8275 ± 0.3875	0.0640 ± 0.0150
$A_n - A_{n-1}$(%)	38.10 ± 3.81	26.94 ± 7.17	24.67 ± 10.20	10.29 ± 0.88
2.0 mM				
k_{appn} (s^{-1})	14.67 ± 0.75	2.585 ± 1.029	0.5445 ± 0.1724	0.0392 ± 0.0112
$A_n - A_{n-1}$(%)	33.26 ± 2.27	30.37 ± 6.20	26.17 ± 7.19	10.20 ± 0.63
1.0 mM				
k_{appn} (s^{-1})	13.67 ± 3.35	2.962 ± 0.972	0.5839 ± 0.0438	0.0557 ± 0.0065
$A_n - A_{n-1}$(%)	25.66 ± 5.29	35.91 ± 5.96	26.44 ± 8.66	11.98 ± 1.07

[a] Mean ± SD with four independent data.

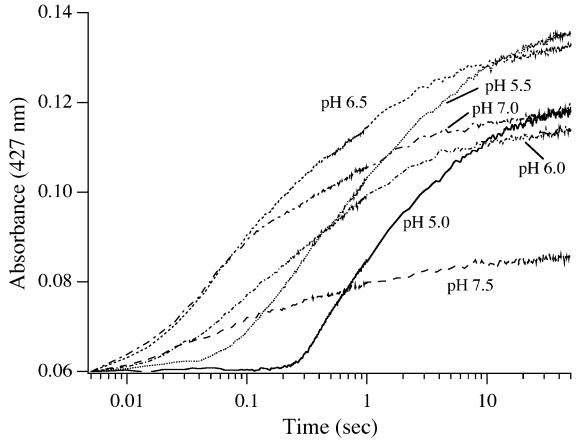

FIGURE 3: pH dependency of the reduction of oxidized cytochrome b_{561} with AsA (2 mM). The stock solution of oxidized cytochrome b_{561} (~300 μM) in 50 mM potassium phosphate (pH 6.0) buffer containing 1.0% octyl β-glucoside was diluted with an appropriate buffer (pH 5.0, 5.5, 6.0, 6.5, 7.0, or 7.5) in a final concentration of 2 μM as described in Materials and Methods. After standing at room temperature for at least 30 min, the sample was mixed with the AsA (4.0 mM) solution (1:1 in volume), and the reduction process was monitored by absorbance change at 427 nm. The time courses are shown on a logarithmic time scale.

might occur. In addition, at a later stage of the reaction, the accumulated MDA radicals might cause oxidation of the reduced heme *b* center on the intravesicular side by direct interaction with the accumulated MDA radicals (*23*). Statistics of the fitted parameters (with four exponential functions) for the reaction of cytochrome b_{561} with various AsA concentrations are tabulated in Table 1. The fastest phase corresponded to about 40% of the total absorbance change at higher AsA concentrations and was reasonably assigned to the first one-electron donation from AsA to the heme *b* center on the extravesicular side. It followed the Michaelis−Menten-type transient kinetics, saturating at high concentrations of AsA. The K_s and k_{+2} values at pH 6.0 were estimated as 2.2 mM and 34.7 s^{-1}, respectively, based on the procedure as described in Materials and Methods.

pH Dependency of Cytochrome b_{561} Reduction with AsA. The effect of pH on the reduction of oxidized cytochrome b_{561} with AsA was examined (from pH 5.0 to 7.5). We found that the time course of the reduction of cytochrome b_{561} was very dependent on the medium pH as shown in Figure 3.

In a higher pH region (pH 7.0 and 7.5), a significant decrease in the final reduction level was observed. Particularly, at pH 7.5, only a half of the heme *b* center was reduced with AsA. This alkaline denaturation occurred very quickly (within 30 min after the preparation of the sample in the alkaline condition for the stopped-flow measurements). This is apparently due to a denaturation of the heme *b* moiety on the intravesicular side, as previously reported for the oxidized cytochrome b_{561} in an alkaline condition (*16*). Indeed, as shown clearly in the Figure 3, the rapid increase of absorbance at 427 nm after the addition of AsA was well conserved at pH 7.5, indicating that the heme *b* center on the extravesicular side was still intact.

Table 2: K_s Values Obtained from the Analyses on the First Reduction Phase[a]

pH	K_s (mM)	k_2 (s^{-1})
7.5[b]	1.15 ± 0.44	17.7 ± 3.7
7.0	4.52 ± 1.75	85.9 ± 31.1
6.5	8.02 ± 0.59	98.0 ± 7.0
6.0	2.18 ± 0.60	34.7 ± 7.5

[a] K_s ($=k_1/k_{-1}$) values were obtained based on the eq 4 as described in the text. [b] The data for pH7.5 were analyzed differently as described in the text, assuming that only the heme *b* center at the extravesicular side could be reduced with AsA.

The K_s and k_{+2} values for pH 6.5 and 7.0 were calculated by the same procedure employed for the analysis of the data obtained at pH 6.0. At pH 7.5, we assumed that only the heme *b* on the extravesicular side could be reduced with AsA as described above and, therefore, the trace could be approximated by comprising only two phases (i.e., a major fast heme *b* reduction phase with AsA and a following minor phase, including the reduction of the residual heme *b* on the intravesicular side and its reoxidation with the accumulated MDA radical). Fittings were satisfactory (data not shown), and the K_s and k_{+2} values were obtained similarly as for pH 6.0. Results were summarized in Table 2.

Reduction of Oxidized Cytochrome b_{561} with AsA in the Acidic pH Region. In a lower-pH region (pH5.0 and 5.5), the reduction process became extremely slow (Figure 3). Further, there was a significant time lag before the reduction of cytochrome b_{561} occurred (Figure 3). However, it must be noted that the final reduction level reached to around 85%, a level similar to those observed at pH 6.0 or 6.5. A representative time course for pH 5.0 is shown on a logarithmic time scale (Figure 4A). The time lag may be interpreted as due to a presence of pH-dependent intermediate(s) before the first electron transfer to heme *b* takes place. To test the feasibility of this scheme, we conducted a simulated fitting to the entire time course according to the

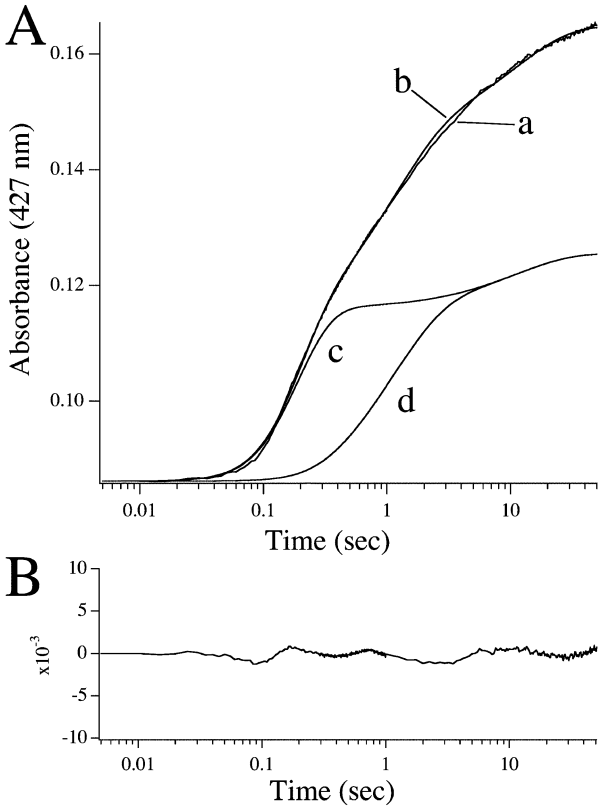

FIGURE 4: Reduction of oxidized cytochrome b_{561} with AsA at pH 5.0. Oxidized cytochrome b_{561} in 50 mM sodium acetate (pH 5.0) buffer containing 1.0% octyl β-glucoside was mixed (1:1 in volume) with sodium AsA (16.0 mM) in the same buffer. Time course of the reduction was followed by absorbance change at 427 nm (trace a) and is shown on a logarithmic time scale (panel A). The observed trace was fitted (trace b) with the extent of the reduction level of two heme centers (i.e., the heme center with a lower redox potential (trace c) and the heme center with a higher one (trace d)) using the procedure described in Materials and Methods. Fitted parameters in panel A are as follows; $k_3' = 19.30\ s^{-1}$, $k_4' = 17.44\ s^{-1}$, $k_5' = 12.02\ s^{-1}$, $k_6' = 0.94\ s^{-1}$, and $k_7' = 0.089\ s^{-1}$, where k_7' is for the slowest single relaxation process as described in the text. In panel B, residual (observed curve *minus* fitted curve) is shown on a logarithmic time scale to clarify the validity of the fitting.

procedure described in MATERIALS AND Methods (equations (5), (7), and (7)′). The fitting was conducted at various AsA concentrations for pH 5.5 and 5.0. We found that at least one intermediate was required before the ES complex (i.e., AsA•b_{561}*) formation to obtain a satisfactory fit (Figure 4A,B). The analysis was extended to the data obtained at higher pH (pH 6.0 and 6.5). Again, the results showed a satisfactory fit with the observed traces (data not shown). The apparent first-order rate constants (k_3', k_4', k_5', and k_6') obtained for eq 7 were plotted against the AsA concentration. Careful analyses of the plots showed that the k_5' followed the hyperbolic nature against the AsA concentration (Figure 5). The plots were analyzed with a least-squares fitting approach, assuming that eq 8 holds. Results were tabulated in Table 3.

Effect of DEPC Treatment on the Electron Transfer from AsA. We analyzed the effect of DEPC treatment on the electron-transfer activity from AsA to oxidized cytochrome b_{561}. At an AsA concentration of 2.0 mM (final) at pH 6.0, oxidized cytochrome b_{561} (1.0 μM) was reduced quickly with the apparent rate constant (k_{app}) of 8.13 s^{-1} for the fastest phase (Figure 6, trace a). The DEPC treatment of the oxidized

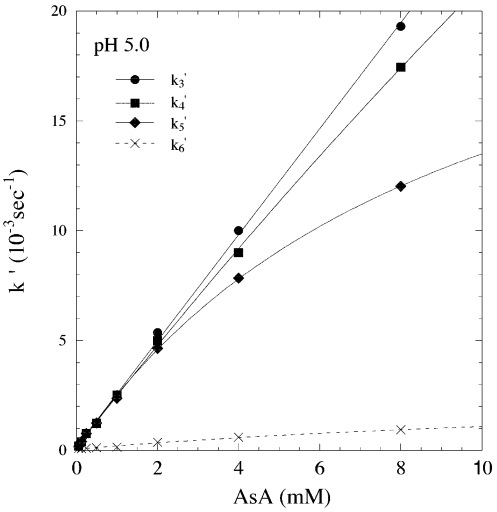

FIGURE 5: Plots of the apparent first-order rate constants (k_3', k_4', k_5', and k_6') of the heme *b* reduction process at the extravesicular side against the AsA concentration measured at pH 5.0. Details are described in the text.

Table 3: Fitted Parameters for the k_5' vs [AsA] Plots for Various pH[a]

pH	C term (=1/(K_3 + K_3K_4))	B term (=k_5K_4/(1 + K_4))
6.5	10.8 ± 3.1	113.3 ± 16.0
6.0	15.0 ± 7.1	72.5 ± 20.3
5.5	12.7 ± 2.6	41.9 ± 5.4
5.0	9.5 ± 0.7	26.4 ± 1.1

[a] Details are described in the text.

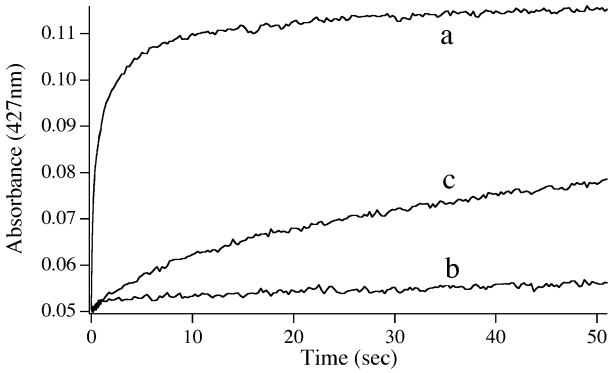

FIGURE 6: Effects of the DEPC treatment of cytochrome b_{561} on the time course of the reduction process with AsA at pH 6.0. Oxidized cytochrome b_{561} in 50 mM potassium phosphate (pH 6.0) buffer containing 1.0% octyl β-glucoside was treated with DEPC (0.5 mM). The DEPC-treated cytochrome b_{561} in the same buffer was mixed (1:1 in volume) with sodium AsA (4.0 mM) in the same buffer. Time course of the reduction was followed by absorbance change at 427 nm (trace b). The DEPC treatment was conducted in the presence of 20 mM AsA, and after oxidation with ferricyanide followed by a gel filtration, the reduction with AsA was monitored (trace c). For a control, reduction process was monitored similarly for the nontreated cytochrome b_{561} (trace a).

cytochrome b_{561} caused an almost complete loss of the first three phases observed for the untreated sample and only the slowest phase remained (Figure 6, trace b). The k_{app} for this phase was estimated to be 0.021 s^{-1}, which was only 1/400 of the fastest phase of the untreated sample. The double reciprocal analyses showed $k_2 = 0.025\ s^{-1}$ for the DEPC-treated cytochrome b_{561}. We have previously shown that a loss of the electron accepting ability from AsA upon the

DEPC treatment was protected by the inclusion of AsA (20 mM) during the treatment (*25*). Present stopped-flow analyses confirmed our previous observation (Figure 6, trace c); the electron-accepting ability from AsA recovered significantly. and the k_{app} for the fastest phase (of the two phases fitted) was estimated to be 0.338 s^{-1}, an increase of 16-fold. The final reduction level reached around 75%, very close to the untreated cytochrome b_{561}. However, it must be noted that the k_{app} value was still only 1/24 of the fastest phase of the untreated sample.

DISCUSSION

In the present study, we conducted a stopped-flow study on the reaction of purified cytochrome b_{561} with AsA for the first time. In the detergent-solubilized state, the hydrophobic surface of cytochrome b_{561} might be shielded with detergent molecules (i.e., octyl β-glucoside), and only two hydrophilic surfaces are exposed to the medium (i.e., extravesicular and intravesicular sides) (*34*−*36*) to allow the access of negatively charged AsA molecules (Figure 1). Since there is one heme *b* center on each side, each heme *b* can receive electron equivalent(s) from AsA but with different affinities and rates. Internal electron-transfer events will also take place. Further, reoxidation of reduced heme *b* center on the intravesicular side with the MDA radical might occur as the reduction level of heme *b* increases. As expected, the observed time course of the reduction of oxidized cytochrome b_{561} with AsA was very complex and could not be fitted with a single exponential (Figure 2A). We found that a linear combination of, at least, four exponential functions was required to obtain an adequate fit (Figure 2A,B). This result was consistent with the notion described above.

The fastest phase was reasonably assigned to the first one-electron donation from AsA to oxidized heme *b* center on the extravesicular side. It followed Michaelis−Menten-type transient kinetics, saturating at high AsA concentrations. The calculated K_s value for AsA (2.2 mM) was slightly lower than the K_m value (∼4 mM) obtained for the chromaffin ghost at pH 6.0 (*32*), but it might be reasonable considering $K_s(= k_{-1}/k_1) < K_m(= (k_{-1}+k_2)/k_1)$. These values were, however, somewhat at variance with the K_m of 0.34 mM at pH 6.5 reported by Flatmark and Terland (*27*). On the other hand, V_{max} values for the heme *b* reduction with AsA were found around 4 s^{-1} for chromaffin ghost (regardless of pH from 5.5 to 7.5) (*32*), which were considerably lower than the corresponding value of k_2 obtained in the present study (Table 2).

We were surprised to observe a significant pH dependency of the reduction process of cytochrome b_{561} when AsA was used as a reductant. In an alkaline region above pH 7.0, the heme *b* center on the intravesicular side was extremely labile, as previously reported (*16*). As a result, only a half of the heme *b* center (i.e., only the heme *b* center on the extravesicular side) could be reduced with AsA at pH 7.5, as shown in Figure 3. It must be noted that the fastest reduction phase, which might be participated by the heme *b* center on the extravesicular side, was fully conserved after the alkaline treatment. This result was fully consistent with our view.

At pH 5.5 and 5.0, we observed a significant time lag before the reduction of heme *b* center occurred (Figures 3 and 4A). The simulated fitting, in which we assumed the presence of a pH-dependent intermediate before the first electron transfer to the heme *b* center on the extravesicular side, was satisfactory as shown in Figure 4A,B. Examination of the results in Table 3 gave us following implications. (a) If the k_5 value was independent of pH (this is a reasonable assumption since this process is actually an intramolecular electron-transfer event), the significant decrease in B-term as pH decrease means the significant decrease in K_4 ($K_4 \ll 1$). This is probably accomplished by a significant decrease in k_4 or significant increase in k_{-4} in the acidic pH region. (b) The decrease in K_4 ($K_4 \ll 1$) in the acidic pH region suggest that the K_3 ($=k_3/k_{-3}$) must be independent of pH. These implications suggest a working hypothesis that a pH-dependent conformational change occurs at the bound AsA moiety before the first electron transfer to the heme *b* center on the extravesicular side takes place. The conformational change may be a gross tertiary structural change or a local conformational change including a deprotonation process from key amino acid residue(s) with pK_a around 5−6 at the AsA-binidng site. Indeed, we had previously proposed that the two histidyl imidazole ligands of the heme *b* center on the extravesicular surface may also participate in the proton acceptor from bound AsA (*25*). The importance of histidyl residues in the electron transfer from AsA to cytochrome b_{561} was also discussed by Njus et al. (*31*, *32*). Unfortunately, however, we do not have appropriate means to discriminate between these two possibilities at present.

In our previous report, we found that the ability of the fast electron acceptance from AsA was completely destroyed by the DEPC treatment of oxidized cytochrome b_{561} (*24*). However, the electron-donating activity from reduced heme *b* to MDA radical was retained (*24*). Three major DEPC-modification sites (His88, His161 and Lys85) were identified by MALDI-TOF mass spectrometric analyses (*24*). The presence of AsA during the DEPC treatment was found to suppress the *N*-carbethoxylation of the heme-coordinating histidyl (His88 and His161) residues, whereas the modification level of Lys85 was not affected (*25*). Concomitantly, the final reduction level of heme *b* with AsA was protected, although the fast reduction process was not fully restored (*25*).

It is obvious that the *N*-carbethoxylation of the heme-coordinating histidyl residues (His88 and His161) on the extravesicular side exerted two apparent effects on the inhibition of the electron transfer from AsA. First, the final reduction level of the total heme *b* decreased to about 35% due to a significant decrease in the midpoint potential of heme *b* on the extravesicular side (*25*). Thus, the heme *b* on the extravesicular side could not be reduced at all with AsA after the DEPC treatment. On the other hand, the heme *b* on the intravesicular side did not suffer so much from the DEPC treatment, and therefore, it could receive electron equivalent from AsA as for the untreated cytochrome b_{561}. Second, the rate of electron transfer from AsA to cytochrome b_{561} decreased remarkably (∼1/400) upon the DEPC treatment (Figure 6). However, in this case, the observed slow heme reduction did not reflect the electron transfer from AsA to the heme *b* on the extravesicular side but was due to the direct electron transfer to the heme *b* center on the intravesicular side. Simultaneously, oxidation of the reduced heme *b* on the intravesicular side by MDA radical just produced by the univalent oxidation of AsA should occur, since this

site has a significant electron donating activity toward MDA radical (*23*). Therefore, the slow reduction of the DEPC-treated cytochrome b_{561} with AsA is actually a reflection of the two opposing effects (i.e., reduction by AsA and oxidation by MDA radical at the heme *b* center on the intravesicular side). Being consistent with this view, the rate constant of this slow reduction was in the same order with that of the slowest phase observed for the untreated cytochrome b_{561} (Figure 2 and Table 1). Further, we found recently that the final reduction level of ~35% of the DEPC-treated cytochrome b_{561} with AsA could be increased up to 50% if MDA radical concentration was decreased in the system by the inclusion of ferrocyanide (Takeuchi et al., unpublished).

Protection from the *N*-carbethoxylation of the heme-coordinating histidyl residues (His88 and His161) but not Lys85 by the inclusion of AsA (20 mM) resulted in a significant restoration of the final reduction level up to 75% (*25*). This fact indicated that heme *b* on the extravesicular side was now reducible with AsA. Further, the reduction rate with AsA was also restored significantly. But it was still only 1/24 of the original rate constant, as shown in Figure 6. Thus, present results clarified the importance of the conserved Lys85 for the interaction with AsA and its indispensable role for the fast electron transfer to the heme *b* center on the extravesicular side.

One may propose that the heterogeneity of the heme center of cytochrome b_{561} can create the complicated kinetics as observed in the present study without introducing a second heme. Although Wimalasena and co-workers (*37*) raised such a possibility on the basis of the alkaline denaturation expreriments, the basis of their claim is rather weak and not consistent with their own observations. However, without a strong piece of evidence such as systematic mutational analysis or X-ray crystallographic analysis, it might be fair to interpret our present results according to the one heme-center model as well. In this case, following conclusions may be made. (1) Requirement of the four exponential functions to fit the observed time course suggested the presence of four distinct cytochrome b_{561} species having a different activity toward AsA (at pH 6.0). (2) At pH 7.5, the major cytochrome b_{561} species that showed a higher activity toward AsA at pH 6.0 hold a similar activity toward AsA but other species seemed to lose their activities almost completely. (3) At pH 5.0 and 5.5, the major cytochrome b_{561} species showed the formation of a distinct transient intermediate before the first electron transfer from AsA to the heme *b* center to occur. (4) DEPC treatment in the oxidized state caused a drastic lowering of the final reduction level (35%) of and the electron-transfer rate (~1/400) from AsA to the single heme center. (5) Inclusion of AsA during the DEPC treatment restored the final reduction level (75%) and the electron-transfer rate (1/24) from AsA to the single heme center.

From our point of views, it seems very difficult to ascribe all these complicated nature of cytochrome b_{561} to the one-heme center. It must be stressed further that genetic evidence for various forms of cytochromes b_{561}, including very distant members of this family such as SDR-2 (*38*), indicated a strict conservation of four His residues. This fact seems to suggest us that the presence of two heme prosthetic groups is a common structural and/or functional requirement among the members of this particular membrane protein family.

In conclusion, we have conducted stopped-flow analyses on the reaction of AsA with cytochrome b_{561} in the solubilized state for the first time. The time course of the reduction of oxidized cytochrome b_{561} with AsA could be fitted with a linear combination of four exponential functions. The fastest phase assignable to the first one-electron donation reaction from AsA to the heme *b* center on the extravesicular side followed the Michaelis−Menten-type transient kinetics with K_s = 2.2 mM (pH 6.0). This fastest phase was completely lost upon a treatment with DEPC in the oxidized state due to the *N*-carbethoxylation of the heme-coordinating histidyl residues (His88 and His161) on the extravesicular side. Presence of AsA during the treatment protected the final reduction level of cytochrome b_{561}, but the reduction rate was still inhibited significantly. This result suggested the importance of the fully conserved Lys85 for the interaction with AsA. At a pH region below 5.5, we observed a significant time lag before the reduction of heme *b* occurred. This time lag was interpreted as due to a pH-dependent transient state before the first electron-transfer reaction to occur.

REFERENCES

1. Rice, M. E. (2000) *Trends Neurosci. 23*, 209−216.
2. Tsukaguchi, H., Tokui, T., Mackenzie, B., Berger, U. V., Chen, X.-Z., Wang, Y., Brubaker, R. F., and Hediger, M. A. (1999) *Nature 399*, 70−75.
3. Eipper, B. A., Mains, R. E., and Glembotski, C. C. (1983) *Proc. Natl. Acad. Sci. U.S.A. 80*, 5144−5148.
4. Kent, U. M., and Fleming, P. J. (1987) *J. Biol. Chem. 262*, 8174−8178.
5. Dhariwal, K. R., Black, C. D. V., and Lavine, M. (1991) *J. Biol. Chem. 266*, 12908−12914.
6. Njus, D., Knoth, J., Cook, C., and Kelley, P. M. (1983) *J. Biol. Chem. 258*, 27−30.
7. Njus, D., Kelley, P. M., and Harnadek, G. J. (1986) *Biochim. Biophys. Acta 853*, 237−265.
8. Wakefield, L. M., Cass, A. E. G., and Radda, G. K. (1986) *J. Biol. Chem. 261*, 9739−9745.
9. Asada, A., Kusakawa, T., Orii, H., Agata, K., Watanabe, K., and Tsubaki, M. (2002) *J. Biochem. 131*, 175−182.
10. Pruss, R. M., and Shepard, E. A. (1987) *Neuroscience 22*, 149−157.
11. Silsand, T., and Flatmark, T. (1974) *Biochim. Biophys. Acta 359*, 257−266.
12. Duong, L. T., and Fleming, P. J. (1982) *J. Biol. Chem. 257*, 8561−8564.
13. Tsubaki, M., Nakayama, M., Okuyama, E., Ichikawa, Y., and Hori, H. (1997) *J. Biol. Chem. 272*, 23206−23210.
14. Burbaev, D. S., Moroz, I. A., Kamensky, Y. A., and Konstantinov, A. A. (1991) *FEBS Lett. 283*, 97−99.
15. Kamensky, Y. A., and Palmer, G. (2001) *FEBS Lett. 491*, 119−122.
16. Okuyama, E., Yamamoto, R., Ichikawa, Y., and Tsubaki, M. (1998) *Biochim. Biophys. Acta 1383*, 269−278.
17. Degli Esposti, M., Kamensky, Y. A., Arutjunjan, A. M., and Konstantinov, A. A. (1989) *FEBS Lett. 254*, 74−78.
18. Srivastava, M., Gibson, K. R., Pollard, H. B., and Fleming, P. J. (1994) *Biochem. J. 303*, 915−921.
19. Srivastava, M. (1996) *DNA Cell Biol. 15*, 1075−1080.
20. Apps, D. K., Boisclair, M. D., Gavine, F. S., and Pettigrew, G. W. (1984) *Biochim. Biophys. Acta 764*, 8−16.
21. Kent, U. M., and Fleming, P. J. (1990) *J. Biol. Chem. 265*, 16422−16427.
22. Kamensky, Y. A., Kulmacz, R. J., and Palmer, G. (2002) *Ann. N.Y. Acad. Sci. 971*, 450−453.
23. Kobayashi, K., Tsubaki, M., and Tagawa, S. (1998) *J. Biol. Chem. 273*, 16038−16042.
24. Tsubaki, M., Kobayashi, K., Ichise, T., Takeuchi, F., and Tagawa, S. (2000) *Biochemistry 39*, 3276−3284.
25. Takeuchi, F., Kobayashi, K., Tagawa, S., and Tsubaki, M. (2001) *Biochemistry 40*, 4067−4076.

26. Dhariwal, K. R., Shirvan, M., and Levine, M. (1991) *J. Biol. Chem. 266*, 5384−5387.
27. Flatmark, T., and Terland, O. (1971) *Biochim. Biophys. Acta 253*, 487−491.
28. Kelley, P. M., and Njus, D. (1988) *J. Biol. Chem. 263*, 3799−3804.
29. Kelley, P. M., Jalukar, V., and Njus, D. (1990) *J. Biol. Chem. 265*, 19409−19413.
30. Jalukar, V., Kelley, P. M., and Njus, D. (1991) *J. Biol. Chem. 266*, 6878−6882.
31. Kipp, B. H., Kelley, P. M., and Njus, D. (2001) *Biochemistry 40*, 3931−3937.
32. Njus, D., Wigle, M., Kelley, P. M., Kipp, B. H., and Schlegel, H. B. (2001) *Biochemistry 40*, 11905−11911.
33. Bernasconi, C. F. (1976) in *Relaxation Kinetics*, Academic Press, New York.
34. Roth, M., Lewit-Bentley, A., Michel, H., Deisenhofer, J., Huber, R., and Oesterhelt, D. (1989) *Nature 340*, 659−662.
35. Michel, H. (1990) in *Crystallization of membrane proteins* (Michel, H., Ed.) pp 73−88, CRC Press, Inc., Boca Raton, FL.
36. le Maire, M., Champeil, P., and Møller, J. V. (2000) *Biochim. Biophys. Acta 1508*, 86−111.
37. Wanduragala, S., Wimalasena, D. S., Haines, D. C., Kahol, P. K., and Wimalasena, K. (2003) *Biochemistry 42*, 3617−3626.
38. Ponting, C. P. (2001) *Hum. Mol. Genet. 10*, 1853−1858.

BI0267588